

Supporting information for

Enhanced charge separation in $\text{CoO}_x@\text{CdS}$ core-shell heterostructure by photodeposited amorphous CoO_x for high efficient hydrogen production

Haorui Liu^{ac*}, Nana Yang^a, Chenchen Feng^{b,c*}, Lei Zhao^a, Ning Mi^a

^a School of Materials Engineering, Longdong University, Qingyang, 745000, Gansu, China

^b State Key Laboratory of Advanced Processing and Recycling of Non-ferrous Metals, Lanzhou University of Technology, Lanzhou, 730050, Gansu, China

^c School of Materials Science and Engineering, Lanzhou University of Technology, Lanzhou, 730050, Gansu, China

1. Characterizations

Zeta potential was performed by was recorded by Litesizer 500. Powder X-ray diffraction (PXRD) data were collected using a Rigaku RINT-2000 X-ray diffractometer with Cu K α radiation ($\lambda=1.54056 \text{ \AA}$), and the tube current and tube voltage was set at 40 mA and 40 kV respectively. Scanning electron microscope (SEM) images were recorded with a Hitachi S4800 FE-SEM system. Transmission electron microscope (TEM) and high-resolution transmission electron microscope (HRTEM) images were obtained by using a JEM1200EX JEOL electron microscope, whose acceleration voltage was set at 100 kV. The Brunauer-Emmett-Teller (BET) method was employed to determine the nitrogen adsorption-desorption isotherm of the samples at 77 K with ASAP 2020. Chemical states of the samples were characterized by X-ray photoelectron spectrometer (a monochromatic Al K α X-ray radiation). UV-vis diffuse reflectance spectra were collected using a Shimadzu UV-2550 spectrometer. The photoluminescence (PL) spectra and time-resolved fluorescence emission spectrum were taken on a Horiba Scientific FluoroMax-4 fluorometer spectrometer at room temperature.

*Corresponding author (email: lhr_tju@163.com)

*Corresponding author (email: fengcc@lut.edu.cn)

2. Detailed electrochemical measurements

Electrochemical measurements were conducted using a CHI-660e workstation (CHI Shanghai, Inc.) with a conventional three-electrode configuration. A platinum wire served as the counter electrode, and a saturated calomel electrode (SCE) functioned as the reference. The working electrodes were fabricated by dispersing 5 mg of photocatalyst and 20 μL of 0.5% Nafion in 1.0 mL ethanol, followed of ultrasonication for 10 min. Then, 50 μL of this dispersion was coated onto cleaned indium tin oxide glass (ITO) substrates ($1\times 1\text{ cm}^2$). The electrodes were subsequently annealed at 100 $^{\circ}\text{C}$ for 1 h. Mott-Schottky analysis was conducted from -0.7 to 2.0 V (vs. SCE) in the dark, applying a 5 mV potential at 1 kHz frequency. Electrochemical impedance spectroscopy (EIS) was performed at 0.5 V vs. SCE, sweeping frequencies from 100 kHz to 0.01 Hz with a 5 mV perturbation. Transient photocurrent responses were captured at 0.2 V vs. SCE under visible light from a 300-W Xe lamp with a 420 nm cutoff filter. The electrocatalytic activity was assessed via linear sweep voltammetry (LSV) at a scan rate of 5 mV s^{-1} .

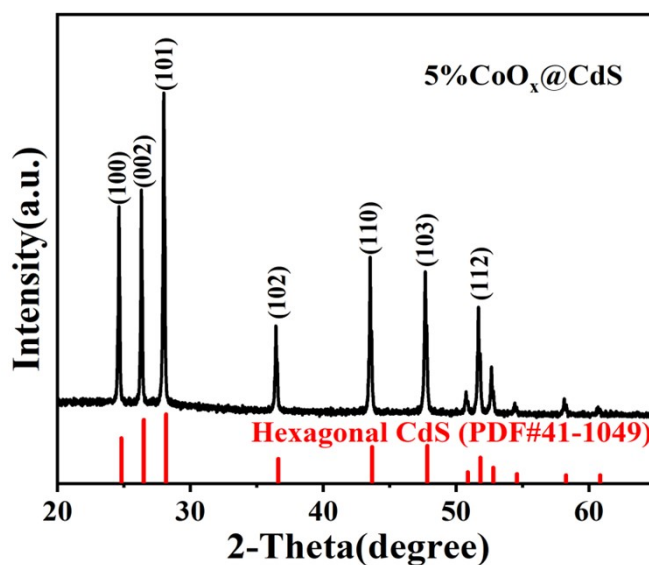


Fig. S1. XRD patterns of 5% CoO_x@CdS sample.

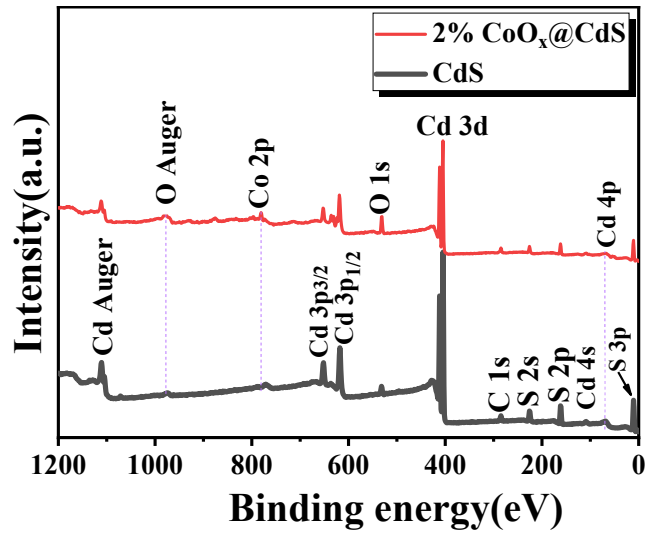
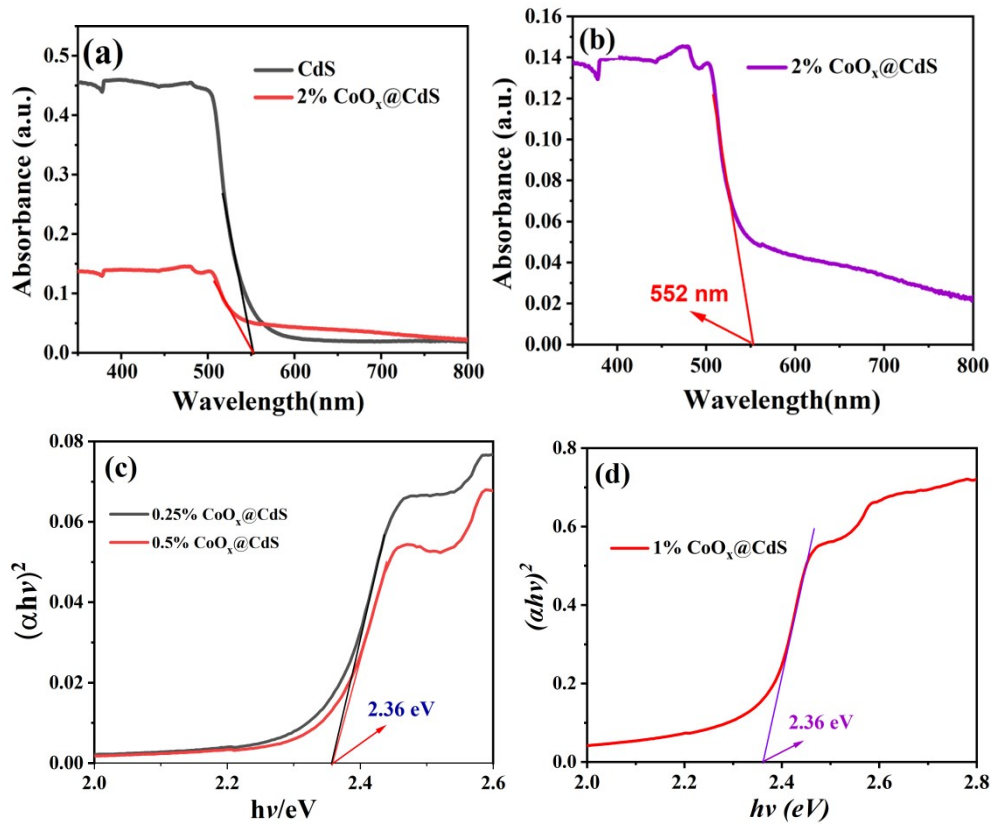


Fig. S2. XPS survey spectra of CdS and 2% CoO_x@CdS sample.



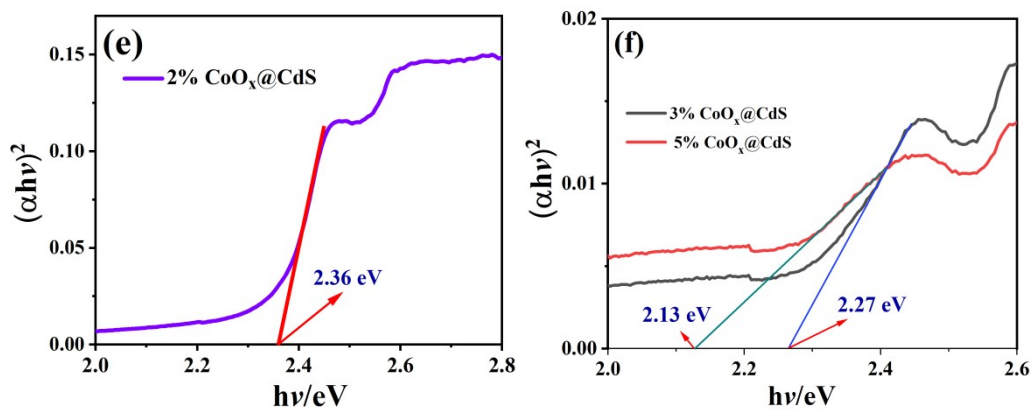


Fig. S3. UV-vis DRS of (a) CdS and 2% CoO_x@CdS samples and (b) 2% CoO_x@CdS; The $(\alpha h\nu)^2$ vs photon energy curves of (c) 0.25% CoO_x@CdS and 0.5% CoO_x@CdS, (d) 1% CoO_x@CdS, (e) 2% CoO_x@CdS, (f) 3% CoO_x@CdS and 5% CoO_x@CdS samples.

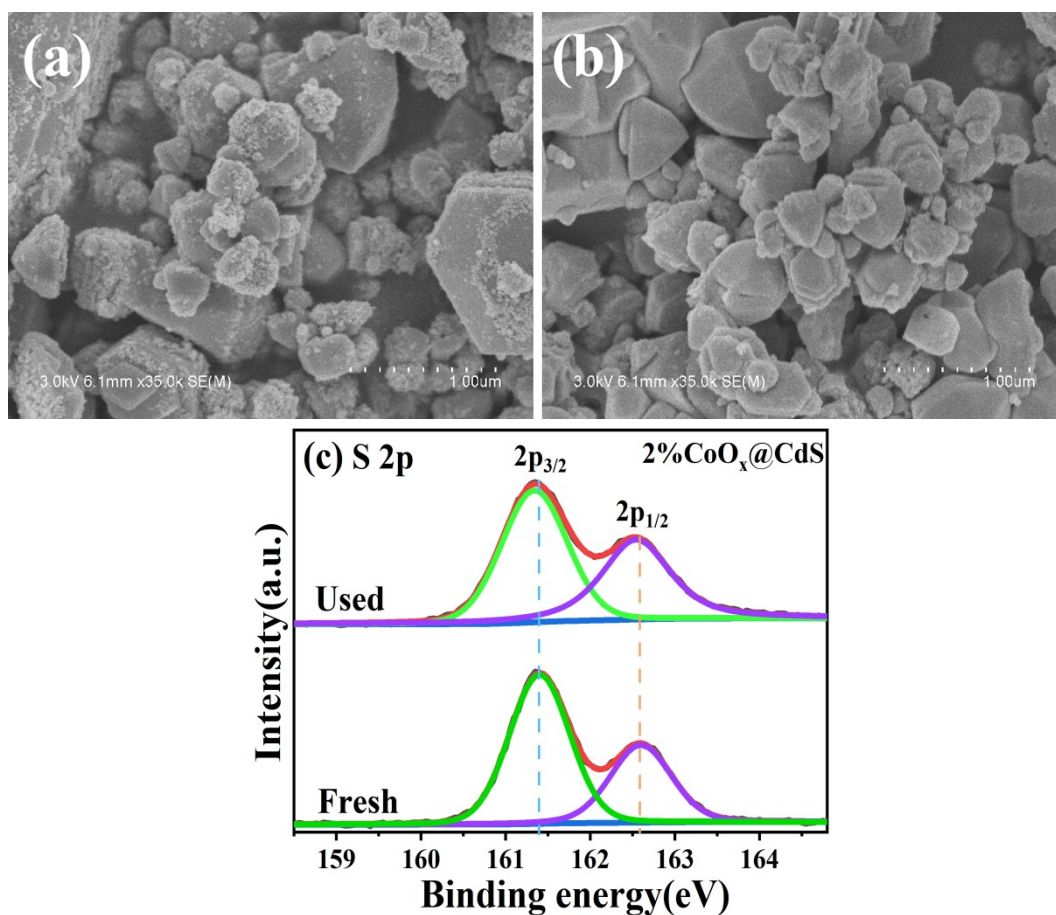


Fig. S4. SEM images of (a) fresh and (b) used 2% CoO_x@CdS samples; (c) XPS spectra of S 2p for the fresh and used 2% CoO_x@CdS samples.

Table S1. Comparison of CdS-based photocatalysts for photocatalytic H₂ production

Photocatalysts	Light sources	Sacrificial reagent	Activity (mmol h ⁻¹ g ⁻¹)	Photostability test time	Ref.
CoO _x /CdS	5 W LED, $\lambda \geq 420$ nm	0.35 M Na ₂ S and 0.25 M Na ₂ SO ₃ (30 mL)	16.30	70 h	This work
CdS/W ₁₈ O ₄₉	300 W Xe lamp with AM-1.5 filter	20v/v%lactic acid (100 mL)	15.4	24 h	1
Co ₃ O ₄ /CdS	300 W Xe lamp	0.25 M Na ₂ SO ₃ /0.35 M Na ₂ S mixed solution (100 mL)	0.62	--	2
WO ₃ /CdS/WS ₂	300 W Xe lamp, $\lambda \geq 420$ nm	lactic acid	14.34	12 h	3
WC/CdS	300 W Xe lamp, $\lambda \geq 420$ nm	lactic acid (10 vol%, 100 mL)	3.31	—	4
Ru, WC/CdS	300 W Xe lamp, $\lambda \geq 420$ nm	lactic acid (10 vol%, 100 mL)	16.8	—	5
CoP/CdS/WS ₂	300 W Xe lamp, $\lambda > 420$ nm	Pure water	0.04	20 h	6
WN/CdS	320 W Xe lamp, $\lambda \geq 420$ nm	lactic acid (10 vol%, 10 mL)	24.13	30	7
CdS/WO ₃	300 W Xe lamp, $\lambda \geq 420$ nm	lactic acid	2.15	—	8

NiS/CdS	300 W Xenon lamp ($\lambda \geq 400$ nm)	lactic acid (3 vol%, 70 mL)	0.55	12 h	9
NiO/CdS	300 W Xenon lamp ($\lambda \geq 420$ nm)	triethanolamine	7.89	--	10
ZnSe/CdS	460 nm LED irradiation	triethylamine	0.38 (4h)	--	11

References

- [1] Y. Xiong, T. Liu, X. Wang, W. Liu, Y. Xue, X. Zhang, C. Xiong, J. Tian, S-scheme heterostructure based on ultrathin 2D CdS coated W18O49 nanosheets-assembled network for highly-efficient photocatalytic H₂ evolution, *J. Alloy. Compd.* 918 (2022) 165652.
- [2] W. Yang, Q. Peng, H. Yang, X. Li, J. Cao, J. Wang, Y. Zheng, C. Li, J. Pan, Hollow Co₃O₄/CdS Nanoparticles for Photocatalytic Hydrogen Evolution and Photodegradation, *ACS Appl. Nano Mater.* 7 (2024) 18157-18166.
- [3] C. Xue, P. Zhang, G. Shao, G. Yang, Effective promotion of spacial charge separation in direct Z-scheme WO₃/CdS/WS₂ tandem heterojunction with enhanced visible-light-driven photocatalytic H₂ evolution, *Chem. Eng. J.* 398 (2020) 125602.
- [4] B. Ma, S. Zhang, W. Wang, L. Feng, R. Zhang, K. Lin, D. Li, H. Zhan, X. Yang, A Novel Earth-Abundant W-WC Heterojunction as Efficient Co-Catalyst for Enhanced Photocatalytic H₂ Evolution, *Chemcatchem*, 12 (2020) 1148-1155.
- [5] K. Lin, L. Feng, D. Li, J. Zhang, W. Wang, B. Ma, Improved photocatalytic hydrogen evolution on (Ru/WC)/CdS via modulating the transferring paths of photo-excited electrons, *Appl. Catal. B Environ.* 286 (2021) 119880,
- [6] Y. Zhong, Y. Wu, B. Chang, Z. Ai, K. Zhang, Y. Shao, L. Zhang, X. Hao, A CoP/CdS/WS₂ p-n-n tandem heterostructure: a novel photocatalyst for hydrogen evolution without using sacrificial agents, *J. Mater. Chem. A*, 7 (2019) 14638,
- [7] H. Liu, J. Chen, W. Guo, Q. Xu, Y. Min, A high efficiency water hydrogen production

method based on CdS/WN composite photocatalytic hydrogen evolution, *J. Colloid Interf. Sci.* 613 (2022) 652-660.

- [8] L. Zhao, X. Chen, Y. Zhang, Z. Ye, Y. Zeng, CdS nanodots adorned (020)-featured $\text{WO}_3 \cdot \text{H}_2\text{O}$ nanoplates heterojunction with augmented photocatalytic hydrogen production under Z-scheme charge transfer mechanism, *J. Environ. Chem. Eng.* 10 (2022) 107612.
- [9] X. Zhang, Y. Zhou, L. Shen, Q. Ou, L. Zhou, S. Jiang, Y. Jia, S. Zhang, H. Wang, Effect of phase of NiS loaded on two-dimensional CdS nanosheets on photocatalytic hydrogen evolution, *J. Molecular Struct.*, 1303 (2024) 137576.
- [10] Y. Lu, Y. Wan, J. Liu, B. Hu, Y. Xie, X. Li, Robust photocatalytic hydrogen evolution performance of 0D/1D NiO/CdS S-scheme heterojunction, *Separation and Purification Technology*, 358 (2025) 130126.
- [11] Z. Qin, L. Shen, S. Yan, J. Wang, Y. Gao, Accumulated photogenerated holes in type-II ZnSe/CdS nanotetrapods for efficient photocatalytic hydrogen evolution, *J. Mater. Chem. A*, 12 (2024) 27641-27651.